PAPER

Catalytic hydroacetylenation of carbodiimides with homoleptic alkaline earth hexamethyldisilazides†

Merle Arrowsmith,[a] Mark R. Crimmin,[b] Michael S. Hill,*[a] Sarah L. Lomas,[a] Myra Sae Heng,[b] Peter B. Hitchcock[c] and Gabriele Kociok-Köhn[a]

The homoleptic alkaline earth hexamethyldisilazides, [M{N(SiMe$_3$)$_2$}$_2$(THF)$_2$] (M = Mg **1a**; Ca **1b**; Sr **1c**), have been shown to act as efficient precatalysts for the hydroacetylenation of organic carbodiimides with alkyl- and arylacetylenes. Catalytic activity was observed to increase with the size of the group 2 metal centre employed and to be strongly influenced by the steric properties of the carbodiimide substrate. The intermediate dimeric calcium and strontium bis(amidinate) complexes, [{PhC≡CC(N^{i}Pr)$_2$}$_2$M]$_2$ (M = Ca **2b**, Sr **2c**), have been isolated and crystallographically characterised. Kinetic studies using the strontium precursor, **1c**, provided a reaction rate law independent of [acetylene] but proportional to [carbodiimide]^2 and inversely proportional to the concentration of the amidine product in solution.

Introduction

The atom-efficient catalytic formation of carbon–carbon bonds is one of the most actively researched areas of modern small molecule synthesis. While transition metal-based processes continue to dominate the field, recent advances have also seen the emergence of a number of non-redox active d^0 metal complexes whose catalytic activity is based on sequences of σ-bond metathesis and polarised insertion of C≡X (X = *e.g.* CR$_2$, O, NR) bonds into a reactive M–C bond.[1] Among d^0 organometallic species, acetylide complexes occupy a privileged position owing to their ease of preparation by protonolysis of metal amide or alkyl precursors with a terminal alkyne. The stoichiometric insertion of polarised multiple bonds (*e.g.* CO$_2$, CS$_2$, R$_2$C=O, RN=C=O, RN=C=S, RC≡N, RN≡C, RN=C=NR) into the M–C bond of rare earth and actinide acetylides is particularly well-documented[2] and ethynylamidinate complexes, synthesised by insertion of carbodiimides into rare earth acetylides, have found numerous applications in catalysis.[3] Several groups have also reported the catalytic hydroacetylenation of carbodiimides using amidocyclopentadienyl-, ethylenebis-(indenyl)-, tethered diamido- and tris(pyrazolyl)-stabilized

trivalent rare earth amide or alkyl precatalysts as well as homoleptic divalent lanthanide precursors.[4] The resulting ethynylamidines, which may not be obtained through hydrolysis of metal amidinate precursors due to their sensitivity to hydrolysis,[4e] have found use as valuable building blocks in the synthesis of more complex organic heterocycles, such as isoxazoles, pyrazoles, pyrroloquinolines and aminoquinolines.[5] In 2006 Richeson and co-workers reported that the commercially available lithium precursor, [Li{N(SiMe$_3$)$_2$}], was also an efficient catalyst for this transformation.[6] In all cases catalysis was shown to proceed *via* the insertion of a carbodiimide molecule into the metal–acetylide bond of the catalyst to form an intermediate ethynylamidinate complex, followed by protonolysis with acetylene to release the ethynylamidine and regenerate the active metal acetylide species as shown in Scheme 1.

In recent years, we and others have developed a rich catalytic chemistry of the relatively inexpensive and earth-abundant
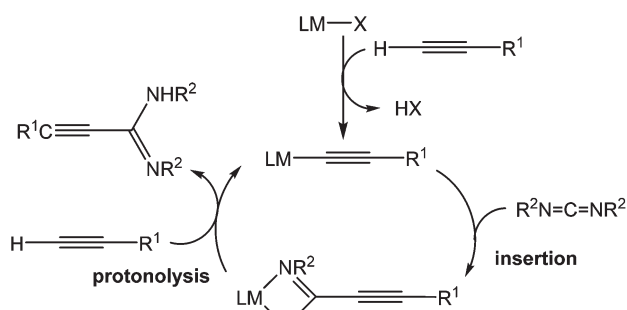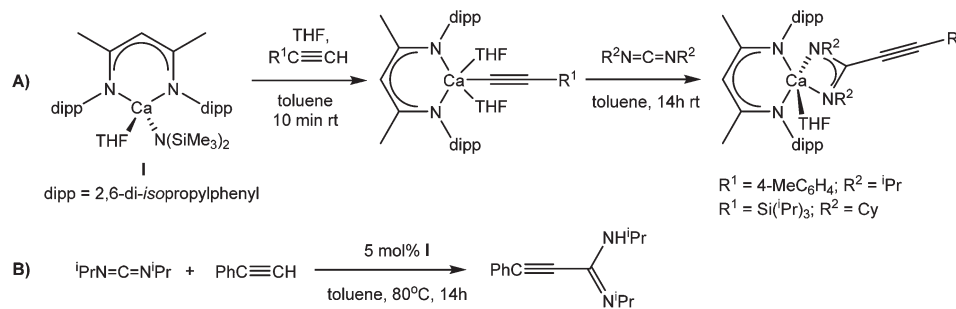
[a] *Department of Chemistry, University of Bath, Claverton Down, Bath, BA2 7AY, UK.*
E-mail: msh27@bath.ac.uk
[b] *Department of Chemistry, Imperial College London, Exhibition Road, South Kensington, London, SW7 2AZ, UK*
[c] *The Chemistry Laboratory, University of Sussex, Falmer, Brighton, BN1 9QJ, UK*
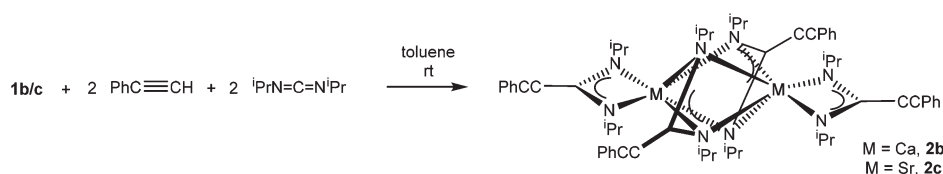
Scheme 1

Scheme 2

heavier alkaline earth metals (Mg, Ca, Sr, Ba) encompassing an ever-increasing variety of heterofunctionalisation, dehydro-coupling and polymerisation reactions.[7] In 2008 we reported the facile stoichiometric insertion of carbodiimides into the calcium–carbon bonds of heteroleptic β-diketiminato calcium acetylide complexes (Scheme 2A).[8] The addition of phenyl-acetylene to N,N'-di-isopropylcarbodiimide was shown to be catalysed by calcium complex **I** at 80 °C in toluene to provide the corresponding N,N'-di-isopropyl-2-phenylethynylamidine in quantitative yield (Scheme 2B). In this case, however, NMR spectroscopic analysis showed that the supporting β-diket-iminate ligand was protonated during the reaction as a result of the acidity of the acetylene substrate. In related work Coles has recently demonstrated that the heteroleptic magnesium amidinate complex, [{MesC(NCy)$_2$}Mg{N(SiMe$_3$)$_2$}(THF)] (Mes = 2,4,6-trimethylphenyl, Cy = cyclohexyl), as well as a number of commercially available magnesium reagents, including MgBu$_2$, [Mg{N(SiMe$_3$)$_2$}$_2$]$_2$, MeMgBr and PhMgBr, may be used to effect the hydroacetylenation of di-isopropyl- and dicyclo-hexylcarbodiimides with a variety of aryl-, alkyl- and trialkyl-silylacetylenes.[9] Herein we report that the series of readily available homoleptic heavier group 2 amide complexes, [M{N-(SiMe$_3$)$_2$}$_2$(THF)$_2$] (M = Mg **1a**; Ca **1b**; Sr **1c**) are also efficient precatalysts for the hydroacetylenation of carbodiimides and provide a study of the reaction mechanism using kinetic analysis.

Stoichiometric studies

Reactions between [M{N(SiMe$_3$)$_2$}$_2$(THF)$_2$] (M = Ca, Sr), two equivalents of N,N'-di-isopropylcarbodiimide and two equi-valents of phenylacetylene in toluene yielded the corresponding alkaline earth bis(N,N'-di-isopropyl-2-phenylethynylamidinate) complexes, **2b** and **2c**, in essentially quantitative yields

(Scheme 3). Colourless single crystals of both compounds were obtained from saturated toluene solutions stored at −30 °C for 24 hours. Details of the X-ray crystallographic analyses are listed in Table 1 while a selection of bond lengths and angles are provided in Table 2 for comparative purposes. In contrast to Coles' monomeric (THF)-solvated magnesium bis(amidi-nate) complex, [{PhC≡CC(N^{i}Pr)$_2$}$_2$Mg(THF)$_2$] (**2a**),[9] both the calcium and strontium analogues, **2b** and **2c**, depicted in Fig. 1, crystallise as homoleptic dimers, in which each group 2 centre is coordinated by one terminal bidentate ethynylamidi-nate ligand and two bridging amidinates. In the case of the larger strontium dication the dimer is centrosymmetric, with the bridging amidinates coordinating to both strontium centres in a (η^2, μ^2) fashion. In contrast, for the smaller calcium dication one of the amidinate ligands bridges in a symmetric (η^2, μ^2) fashion to both metal centres, while the other bridges asymmetrically, coordinating to the six-coordi-nate Ca(1) centre through both N(5) and N(6), and to the five-coordinate Ca(2) centre via N(6) only. Several trends can be dis-cerned over the series of homoleptic complexes **2a–2c**. The metal–nitrogen bond lengths to the terminal ethynylamidinate ligands increase gradually with the size of the metal centre from magnesium in **2a** (*ca.* 2.17 Å) to strontium in **2c** (*ca.* 2.53 Å). The N–C–N angles of both the terminal and brid-ging ligands increase by *ca.* 2° from **2a** to **2c** in order to accom-modate the larger metal centres while the N–M–N bite angles decrease by *ca.* 5.4° from **2a** to **2b** and *ca.* 3.5° from **2b** to **2c**, in line with the more significant cationic radius increase between magnesium and calcium. The Ca–N bond lengths to the terminal amidinate ligands in complex **2b** [2.367(3)–2.382(2) Å] are significantly shorter than those observed in our pre-viously reported heteroleptic N,N'-di-isopropyl-2-p-tolylethynyl-amidinate complex [2.3918(14), 2.4294(14) Å], which may be ascribed to the high steric demands of the β-diketiminate co-ligand in the latter species.[8] Due to the coordination to both

Scheme 3

Table 1 Details of X-ray crystallographic analyses for compounds **2b**, **2c**, **3** and **4**

	2b	**2c**	**3**	**4**
Formula	$C_{60}H_{76}Ca_2N_8$	$C_{60}H_{76}N_8Sr_2$	$C_{45}H_{57}BaKN_6$	$C_{33}H_{40}N_2 \cdot C_6H_6$
M_w	989.45	1084.53	858.41	542.78
T (K)	173(2)	173(2)	150(2)	150(2)
Crystal system	Triclinic	Monoclinic	Monoclinic	Monoclinic
Space group	$P\bar{1}$	$P2_1/c$	$C2/c$	$C2/c$
a (Å)	10.8208(3)	12.9424(2)	26.4080(3)	22.5370(2)
b (Å)	16.1524(4)	19.6115(4)	16.4240(2)	12.92390(10)
c (Å)	17.4648(3)	11.7596(3)	21.1240(3)	25.3579(3)
α (°)	96.295(2)	90	90.00	90
β (°)	94.289(1)	98.832(1)	97.322(1)	115.4780(4)
γ (°)	93.976(1)	90	90.00	90
V (Å³)	3016.36(12)	2949.43(11)	9087.3(2)	6667.62(11)
Z	2	2	8	8
ρ (mg m⁻³)	1.09	1.22	1.255	1.081
μ (mm⁻¹)	0.23	1.851	1.001	0.062
θ range (°)	3.53 to 26.05	3.50 to 26.05	3.62 to 27.48	3.560 to 25.096
Reflections measured	42 730	39 387	92 722	48 040
Independent reflections	11 828	5802	10 399	48 040
R_{int}	0.0417	0.0612	0.0984	—
Final R_1 values ($I > 2\sigma(I)$)	0.0716	0.0348	0.0384	0.0645
Final $wR(F^2)$ values ($I > 2\sigma(I)$)	0.1857	0.0749	0.0675	0.1364
Final R_1 values (all data)	0.1012	0.0496	0.0799	0.0826
Final $wR(F^2)$ values (all data)	0.2077	0.0807	0.0788	0.1473

Table 2 Selected bond lengths (Å) and angles (°) for compounds **2b**, **2c**, **3** and **4**

	2b[a]	**2c**[b]	**3**[c]	**4**
$[M–N]_t$	2.382(2), 2.370(3), 2.371(3), 2.367(3)	2.527(2), 2.551(2)	—	—
$[M–N]_{a.b.}$	2.361(3), 2.733(3)	—	2.760(2),[d] 2.808(2),[d] 2.759(2),[d] 2.820(2)[d]	—
$[M–N]_{s.b.}$	2.650(3), 2.464(2)	2.751(2), 2.668(2)	2.789(2),[e] 2.897(2)[e]	—
$[M'–N]_{a.b.}$	3.448(3), 2.404(3)	—	3.178(2),[d] 2.914(2),[d] 2.891(2),[d] 2.955(2)[d]	—
$[M'–N]_{s.b.}$	2.445(3), 2.602(2)	2.723(2), 2.732(2)	2.936(2),[e] 3.036(2)[e]	—
$[N–C]_t$	1.333(4), 1.327(4), 1.332(4), 1.320(5)	1.335(3), 1.321(3)	—	1.325(3), 1.326(3)
$[N–C]_{a.b.}$	1.428(5), 1.242(4)	—	1.332(4),[d] 1.331(4)[d] 1.334(4),[d] 1.332(4)	—
$[N–C]_{s.b.}$	1.324(4), 1.331(4)	1.338(3), 1.334(3)	1.336(3),[e] 1.332(3)[e]	—
$[N–M–N]_t$	57.31(8), 57.27(10)	53.56(6)	—	—
$[N–M–N]_{a.b.}$	51.84(12)	—	48.53(7),[d] 48.46(7)[d]	—
$[N–M–N]_{s.b.}$	52.04(8)	49.75(6)	47.38(6)[e]	—
$[N–M'–N]_{a.b.}$	40.54(9)	—	43.86(6),[d] 46.11(7)[d]	—
$[N–M'–N]_{s.b.}$	52.83(8)	49.42(6)	44.99(6)[e]	—
$[N–C–N]_t$	117.9(3)	118.9(2)	—	119.3(2)
$[N–C–N]_{a.b.}$	114.9(3)	—	118.6(2),[d] 118.4(2)[d]	—
$[N–C–N]_{s.b.}$	115.9(3)	117.2(2)	117.9(2)[e]	—

[a] M/M' = Ca. [b] M/M' = Sr. [c] M = Ba, M' = K. [d] N(1) to N(4). [e] N(5)/N(6); t = terminal; $a.b.$ = asymmetric bridging; $s.b.$ = symmetric bridging.

calcium centres the Ca–N bonds of the symmetrically bridging ligand in **2b** are significantly elongated [2.445(3)–2.650(3) Å] while the corresponding N–Ca–N bite angles [ca. 52.5°] are considerably smaller than those of the terminal ligands [ca. 57.3°]. For the asymmetrically bridging ethynylamidinate ligand, the Ca(1)–N(5) [2.361(3) Å] and Ca(2)–N(6) bond lengths [2.404(3) Å] are within the range of those observed for terminal calcium amidinate ligands, whereas the Ca(1)–N(6) bond is lengthened to 2.733(3) Å. A similar symmetric/asymmetric bridging motif has been observed for the related strontium bis(N,N'-di-isopropyl-N'',N''-dimethylguanidinate) dimer

reported by Cameron and co-workers.[10] Conversely the strontium dimer, **2c**, exhibits two (η^2, μ^2) bridging ligands, in a similar fashion to the analogous strontium bis(N,N',N'',N''-tetra-isopropylguanidinate) dimer reported by the same authors; in this latter case, however, the Sr–N distances are somewhat longer and the N–Sr–N angles slightly more acute than in **2c** due to the higher steric demands of the di-isopropyl-amido ligand backbone substituents.

NMR studies of complexes **2b** and **2c** showed that the compounds retain their solid-state nuclearity in solution at room temperature. ¹H and ¹³C NMR spectra for both compounds
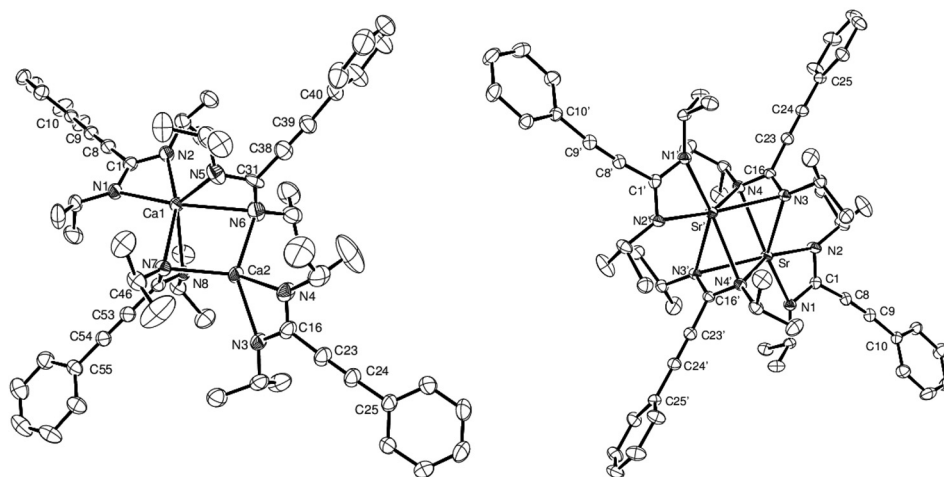
Fig. 1 ORTEP representations of the calcium and strontium bis(ethynylamidinate), complexes **2b** (left) and **2c** (right). Thermal ellipsoids drawn at 30% probability. Hydrogen atoms removed for clarity.

displayed two distinct sets of resonances for the terminal and bridging ethynylamidinate ligands at room temperature. Whereas the isopropyl ^{1}H NMR resonances of **2b** were well-defined, those of **2c** remained broad until cooled to 238 K, indicating some fluxional behaviour presumably caused by the greater degree of conformational freedom around the larger strontium centres. The ^{13}C resonances of the metallacyclic carbon [**2b** δ 160.4, 158.5 ppm; **2c** δ 158.8, 158.6 ppm] are very similar to that reported for the analogous monomeric magnesium complex.[9]

Attempts to isolate the analogous homoleptic barium N,N'-di-isopropyl-2-phenylethynylamidinate by the same route invariably yielded the polymeric mixed barium–potassium complex, $[\{PhC\equiv CC(N^iPr)_2\}_3BaK]_n$, compound **3**, which was identified by a single crystal X-ray diffraction analysis. The results of this experiment are shown in Fig. 2, while details of

the analysis and selected bond length and angle data are provided in Tables 1 and 2, respectively. Compound **3** crystallises as a 1-dimensional polymer propagated by η^2–μ^2-interactions between alternate barium and potassium centres and the amidinate ligands. While the bimetallic assembly of **3** is unprecedented for an amidinate-based system, the Ba–N bond distances [2.759(2)–2.897(2) Å] observed within the structure for the Ba–N–K bridging amidinate linkages are significantly elongated in comparison to the terminal Ba–N bonds observed in the only previously reported barium amidinate, a 6-coordinate monometallic species containing chelating N,N'-bis(2,6-di-isopropylphenyl)formamidinate ligands [Ba–N 2.685(3)–2.769(3) Å].[11] The structure of compound **3** suggests that the barium bis(hexamethyldisilazide) starting material was heavily contaminated with the $[BaK\{N(SiMe_3)_2\}_3]$ 'ate' complex and closer analysis of the supposed barium
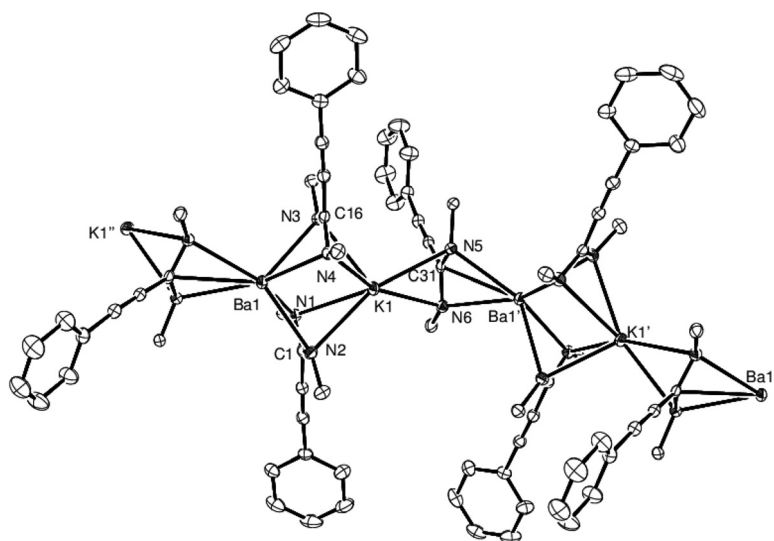

Fig. 2 ORTEP representation of polymeric complex 3. Thermal ellipsoids drawn at 30% probability. Hydrogen atoms and isopropyl methyl groups omitted for clarity. Symmetry transformations used to generate equivalent atoms: #1 −x + 1/2, y − 1/2, −z + 1/2 #2 −x + 1/2, y + 1/2, −z + 1/2.

bis(hexamethyldisilazide) starting material revealed a *ca.* 1 : 10 ratio of the desired [Ba{N(SiMe$_3$)$_2$}$_2$(THF)$_2$] and [BaK{N-(SiMe$_3$)$_2$}$_3$], the mixture being virtually undistinguishable by NMR spectroscopy from the solvent-free complex, [Ba{N-(SiMe$_3$)$_2$}$_2$]$_2$. Repeated attempts with different batches of the barium precursor, obtained by salt metathesis from barium iodide and potassium hexamethyldisilazide in THF, yielded the same result, demonstrating the unreliability of this route for the synthesis of pure [Ba{N(SiMe$_3$)$_2$}$_2$(THF)$_2$].
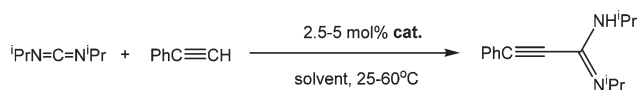
Catalytic studies

Complexes **1a–1c** (5 mol%) were screened for their efficacy in the catalytic hydroacetylenation of *N,N′*-di-isopropylcarbodiimide with phenylacetylene at room temperature (Scheme 4). The magnesium complex, **1a** (Table 3, entry 1), displayed higher activity than the heteroleptic magnesium amidinate complex, [{MesC(NCy)$_2$}Mg{N(SiMe$_3$)$_2$}(THF)], which only provided 44% conversion after 24 h at room temperature, with a catalyst loading of 10 mol%.[9] NMR yields after 24 hours showed increased conversion with increasing size of the alkaline earth metal dication used (entries 1–3). The barium 'ate' complex, [BaK{N(SiMe$_3$)$_2$}$_3$], displayed even higher activity than the strontium precursor, **1c** (entry 4). In subsequent catalytic and mechanistic studies, however, the latter precatalyst was used to provide a more well-defined system. A similar trend of increasing activity with increasing cation size was observed by Zhou and co-workers when comparing the homoleptic rare earth(II) hexamethyldisilazide precatalysts, [M{N(SiMe$_3$)$_2$}$_2$-(THF)$_3$] (M = Sm, Eu, Yb), for the same reaction.[4c]

In all cases a marked product inhibition effect was observed, as well as an increase in reactivity when performing the reaction in a 9 : 1 mixture of C$_6$D$_6$ and d$_8$-THF using the calcium and strontium precatalysts, **1b** and **1c**. Performing the reaction in d$_8$-THF alone did not provide any significant improvement in reactivity. Zhou and co-workers have reported
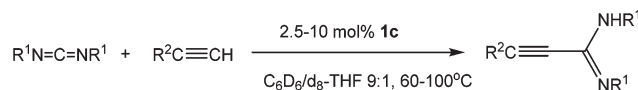
similarly improved catalytic activity upon addition of donor THF over a range of rare earth precatalysts.[4] In contrast, and as already observed by Coles,[9] the magnesium-catalysed reaction was significantly impeded by the addition of THF. It is therefore likely that the increased reactivity of **1b** and **1c** in the presence of small amount of THF is the result of the breakup of the bis(ethynylamidinate) dimers, **2b** and **2c**, to form catalytically-active monomeric THF-solvated calcium and strontium bis(amidinates) similar to **2a**.

The substrate scope of the reaction was examined using precatalyst **1c** in a 9 : 1 mixture of C$_6$D$_6$ and d$_8$-THF (Scheme 5). As expected, the increase in steric demands of the carbodiimide *N*-substituents caused a drastic drop in reactivity in the order of ^{i}Pr ≈ Cy > ^{t}Bu ≫ 2,6-^{i}Pr$_2$C$_6$H$_3$ (Table 4, entries 1–4) as previously observed by Schwamm and Coles.[9] It is notable that this is the first report of catalytic hydroacetylenation for highly hindered carbodiimides such as the *tert*-butyl and the 2,6-diisopropylphenyl derivatives. Colourless single crystals of *N,N′*-bis(2,6-di-isopropylphenyl)-2-phenylethynylamidine, compound **4**, were obtained from the NMR scale reaction in C$_6$D$_6$–THF 9 : 1 at 4 °C. In contrast to other isolated 2-ethynylamidine compounds, which have been shown to be prone to hydrolysis, the latter compound was air- and moisture-stable, presumably a consequence of the steric shielding provided by the large *N*-aryl groups. Compound **4**, as deduced by a single crystal X-ray diffraction analysis (Fig. 3; details of X-ray analysis and selected bond length and angle data are presented in Tables 1 and 2), crystallises as the *cis* isomer with respect to the C=N bond and forms hydrogen-bonded dimers [N(1′)–H(1) 1.95(6), N(2)–H(2′) 1.99(7) Å]. Both the C(1)–N(1) and C(1)–N(2) bond lengths [1.325(3) and 1.326(3) Å] are intermediate between formal C–N single and C=N double bonds due to the amino proton being equally disordered over both nitrogen atoms.

The catalytic reactions were also found to be sensitive to the nature of the acetylene substituent, with aryl functionalities requiring lower reaction temperatures (entries 1 and 8)

^{i}PrN=C=N^{i}Pr   +   PhC≡CH $\xrightarrow[\text{solvent, 25-60°C}]{\text{2.5-5 mol% cat.}}$ PhC≡C–C(NH^{i}Pr)=N^{i}Pr

Scheme 4

R^{1}N=C=NR^1 +   R^{2}C≡CH $\xrightarrow[\text{C}_6\text{D}_6/\text{d}_8\text{-THF 9:1, 60-100°C}]{\text{2.5-10 mol% 1c}}$ R^{2}C≡C–C(NHR^1)=NR^1

Scheme 5

Table 3 Catalyst and solvent screening for the catalytic hydroacetylenation of carbodiimides

Entry	R^1	R^2	Catalyst (mol%)	Solvent	Time (h)	Temp. (°C)	NMR yield[a] (%)
1	^{i}Pr	Ph	**1a** (5.0)	C$_6$D$_6$	24	25	61
2	^{i}Pr	Ph	**1b** (5.0)	C$_6$D$_6$	24	25	66
3	^{i}Pr	Ph	**1c** (5.0)	C$_6$D$_6$	24	25	79
4	^{i}Pr	Ph	[BaK{N(SiMe$_3$)$_2$}$_3$] (5.0)	C$_6$D$_6$	24	25	89
5	^{i}Pr	Ph	**1c** (2.5)	C$_6$D$_6$	0.5	25	6
6	^{i}Pr	Ph	**1c** (2.5)	C$_6$D$_6$–d$_8$-THF 9 : 1	0.5	25	28
7	^{i}Pr	Ph	**1c** (2.5)	d$_8$-THF	0.5	25	25
8	^{i}Pr	Ph	**1c** (2.5)	C$_6$D$_6$–d$_8$-THF 9 : 1	18	60	93

[a] Measured by integration against bis(trimethylsilyl)amine released from catalyst activation.

Table 4 Scope of carbodiimide hydroacetylation in C_6D_6–d_8-THF 9 : 1

Entry	R^1	R^2	Cat. (mol%)	Time (h)	Temp. (°C)	NMR yield[a,b] (%)
1	^iPr	Ph	**1c** (2.5)	18	60	93 (98)
2	Cy	Ph	**1c** (2.5)	18	60	94 (99)
3	^tBu	Ph	**1c** (5.0)	18	100	84 (94)
4	2,6-$^iPr_2C_6H_3$	Ph	**1c** (10.0)	48	100	71 (91)
5	^iPr	^nBu	**1c** (5.0)	18	80	72 (82)
6	Ph	Cy	**1c** (5.0)	24	80	73 (83)
7	Ph	^tBu	**1c** (5.0)	48	100	79 (89)
8	Ph	4-MeC_6H_4	**1c** (2.5)	18	60	78 (83)
9	Ph	CH_2NMe_2	**1a** (5.0)	48	80	77 (87)
10	Ph	CH_2OMe	**1a** (5.0)	48	80	74 (84)

[a] Measured by integration against bis(trimethylsilyl)amine released from catalyst activation. [b] Yield of free amidine (in parentheses: NMR yield after hydrolysis with a few drops of D_2O).
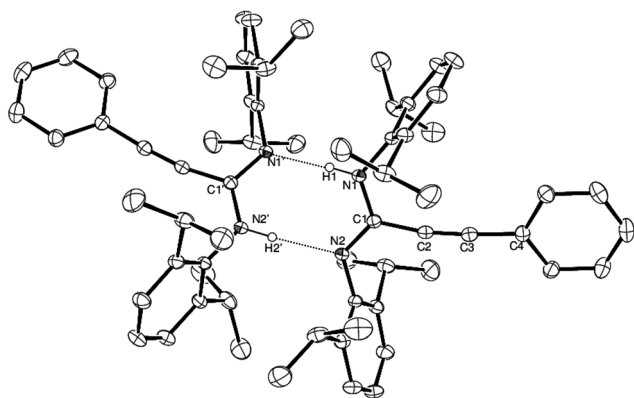

Fig. 3 ORTEP representation of the hydroacetylation product of *N*,*N*′-bis(2,6-di-isopropylphenyl)carbodiimide with phenylacetylene, compound **4**. Thermal ellipsoids drawn at 30% probability. Hydrogen atoms removed for clarity except for the amino proton, H(1) and H(2)′. Hydrogen bonds drawn as dashed bonds.

than alkyl functionalities (entries 5–7 and 9–10) to reach completion. A significant steric effect of the acetylene functional group was only observed for the largest substrate, *tert*-butylacetylene, which required forcing conditions and long reaction times to achieve good conversions (entry 7). In all catalytic reactions the intermediate strontium bis(ethynylamidinate) complex was observed by ^1H NMR spectroscopy throughout the course of the reaction and remained visible in solution after consumption of all substrates. At this point addition of a few drops of D_2O to the reaction mixture enabled the liberation of two further equivalents of the amidine product per strontium centre (see yields in parentheses in Table 4). The NMR resonances of the intermediate strontium bis(amidinate) complex also suggested a monomeric species analogous to the magnesium complex, **2a**, rather than the dimeric structure of **2c**. This is likely the result of the large excess of THF solvent, which stabilises the monomeric species during catalysis. With donor-functionalised propargyl substrates, such as methylpropargyl ether and 3-(*N*,*N*-dimethylamino)-1-propyne, which are known to undergo dimerisation in the presence of group 2 bis(amido) precatalysts,[12] competitive acetylene dimerisation and carbodiimide hydroacetylation were observed when

using the calcium and strontium precatalysts, **1b** and **1c**. In contrast the magnesium precursor **1a** yielded the corresponding propargylamidines cleanly at reaction temperatures up to 80 °C, above which negligible amounts of the butatriene product were observed (entries 9 and 10). The presence of the potentially coordinating methoxy and dimethylamino moieties also suppressed the reaction rate compared to the analogous reaction with 1-hexyne.

Mechanistic studies

Kinetic analysis of a NMR scale reaction ([PhC≡CH] = [^iPrN=C=N^iPr] = 0.04 M, [**1b**] = 8 mM) performed at 60 °C revealed *pseudo*-second-order kinetics over a period of three half-lives, with an apparent rate constant of k_H = 0.15 min M^{-1}. An identical experiment but using 1-deuterophenylacetylene, PhC≡CD, yielded an apparent rate constant of k_D = 0.19 min M^{-1}, providing a negligible kinetic isotope effect of 1.23 (Fig. 4, left). Protonolysis of the amidinate complex by the acetylene is therefore unlikely to be rate-determining in the catalytic cycle. A further kinetic experiment performed with 10 molar equivalents of phenylacetylene per carbodiimide yielded a *pseudo* second-order reaction in [^iPrN=C=N^iPr] over three half-lives, confirming that phenylacetylene is not involved in the rate-determining step (Fig. 4, right). The latter process was, therefore, deduced to be the insertion of the carbodiimide into the strontium acetylide bond. Irrespective of this apparent independence of reaction rate upon [PhC≡CH]$_t$ the apparent rate constant was observed to experience a 10-fold increase under these conditions, from 0.15 to 1.90 min M^{-1}, suggesting a dependence of reaction rate on the initial concentration of acetylene, [PhC≡CH]$_0$. Conversely performing the reaction in the presence of the amidine product led to a drastic rate decrease. We suggest that this observation is most likely due to competitive protonolysis of the strontium amidinate intermediate by the amidine product itself rather than by the acetylene substrate. A plot of the rate constants *versus* five different inverse initial amidine concentrations provided a linear correlation (Fig. 5, left, see Fig. S2 in ESI† for corresponding kinetic analyses). Furthermore a series of
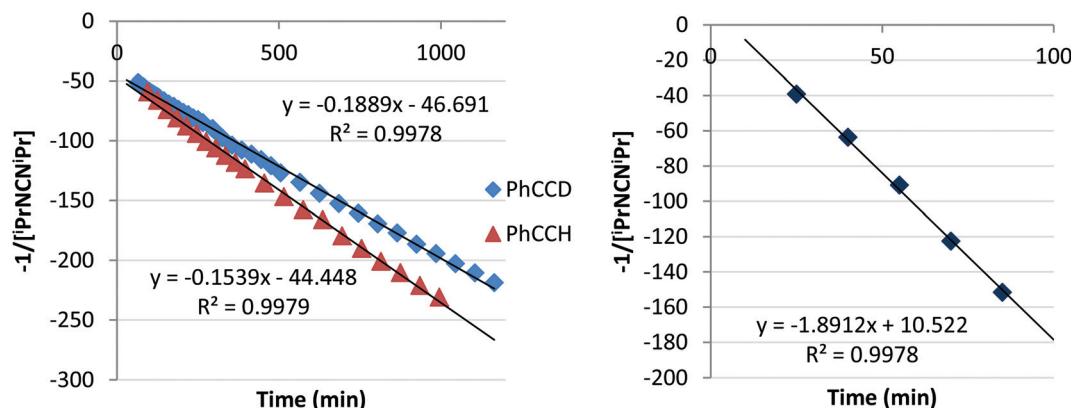
Fig. 4 *Left*: 2nd-order kinetic analysis of the NMR scale reaction of phenylacetylene or 1-deuterophenylacetylene (0.04 M) and di-isopropylcarbodiimide (0.04 M) in 0.5 mL of C_6D_6–d_8-THF 9:1 with 2.5 mol% of **1c** at 60 °C. *Right*: 2nd-order kinetic analysis of the reaction of 10 molar equivalents of phenylacetylene (0.4 M) and di-isopropylcarbodiimide (0.04 M) in 0.5 mL of C_6D_6–d_8-THF 9:1 with 2.5 mol% of **1c** at 60 °C.
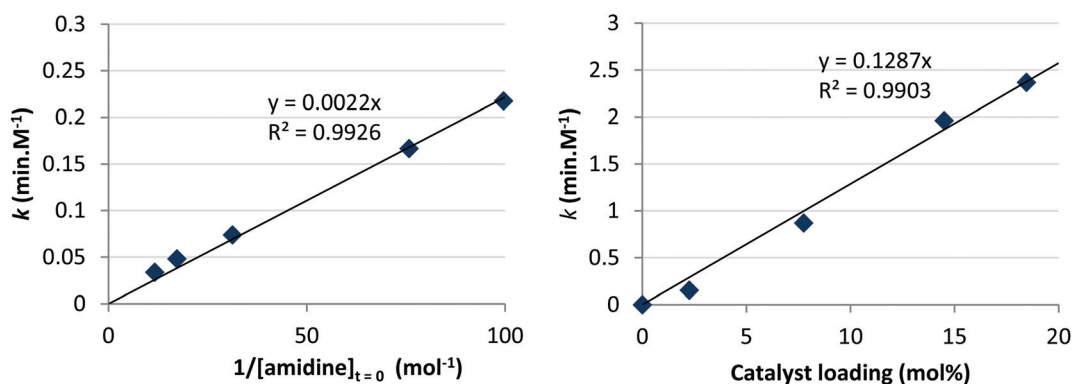

Fig. 5 *Left*: Linear correlation between the apparent rate constant k (min M^{-1}) and $1/[\text{amidine}]_{t=0}$ (mol^{-1}) for kinetic runs performed in 0.5 mL of C_6D_6–d_8-THF 9:1 with 2.5 mol% of **1c** at 60 °C. *Right*: Linear correlation between the apparent rate constant k (min M^{-1}) and catalyst loading (%) using a 0.04 M mixture of phenylacetylene and di-isopropylcarbodiimide in 0.5 mL of C_6D_6–d_8-THF 9:1 at 60 °C.

experiments conducted at increasing catalyst loading while maintaining the substrate concentration at 0.04 M yielded a first-order plot in [**1c**] (Fig. 5, right, see Fig. S2 in ESI† for corresponding kinetic analyses), supporting the participation of a monomeric THF-supported strontium bis(amidinate) complex, which is present throughout the course of the catalytic reaction (*vide supra*).

The rate of reaction can thus be expressed as:

$$\frac{d[\text{CDI}]}{dt} = -k[\text{RCCH}]_0[\textbf{1c}]\frac{[\text{CDI}]^2}{[\text{amidine}]} \quad (\text{CDI} = \text{carbodiimide})$$

Conclusion

Simple THF-solvated magnesium, calcium and strontium bis-(bis(trimethylsilylamide)) complexes have been assessed as precatalysts for the hydroacetylenation of carbodiimides. The strontium precursor proved to be the most efficient precatalyst, providing good yields of the desired amidines even for the most hindered carbodiimide substrates. Kinetic analyses revealed that carbodiimide insertion provides the rate-limiting

step and that the reactions are self-inhibiting. We are currently assessing the use of these amidines as synthons for further group 2 catalysed functionalisation reactions and will report our findings in due course.

Acknowledgements

References

1 For a selection of recent publications in the field, see: (*a*) B. T. Guan, B. Wang, M. Nishiura and Z. Hou, *Angew. Chem., Int. Ed.*, 2013, **52**, 4418; (*b*) J. Oyamada and Z. Hou, *Angew. Chem., Int. Ed.*, 2012, **51**, 12828; (*c*) B. T. Guan and Z. Hou, *J. Am. Chem. Soc.*, 2011, **133**, 18086; (*d*) R. Kubiak, I. Prochnow and S. Doye, *Angew. Chem., Int. Ed.*, 2009, **48**, 1153; (*e*) A. D. Sadow and T. D. Tilley, *J. Am. Chem. Soc.*, 2003, **125**, 7971. For a selection of recent reviews on the subject, see: (*f*) S. Kobayashi and Y. Yamashita, *Acc. Chem.*

Res., 2011, **44**, 58; (*g*) K. C. Hultzsch and A. L. Reznichenko, Catalytic σ-Bond Metathesis, in *Structure and Bonding*, ed. P. W. Roesky, Springer, 2010, vol. 137, p. 1; (*h*) U. Rosenthal, V. V. Burlakov, M. A. Bach and T. Beweries, *Chem. Soc. Rev.*, 2007, **36**, 719; (*i*) U. Rosenthal, P. Arndt, W. Baumann, V. V. Burlakov and A. Spannenberg, *J. Organomet. Chem.*, 2003, **670**, 84; (*j*) M. Shibasaki and N. Yoshikawa, *Chem. Rev.*, 2002, **102**, 2187; (*k*) J. Inanaga, H. Furuno and T. Hayano, *Chem. Rev.*, 2002, **102**, 2211.

2 (*a*) I. J. Casely, J. W. Ziller and W. J. Evans, *Organometallics*, 2011, **30**, 4873; (*b*) E. M. Matson, P. E. Fanwick and S. C. Bart, *Organometallics*, 2011, **30**, 5753; (*c*) W. Yi, J. Zhang, M. Li, Z. Chen and X. Zhou, *Inorg. Chem.*, 2011, **50**, 11813; (*d*) M. L. Cole, G. B. Deacon, C. M. Forsyth, P. C. Junk, D. Polo Ceron and J. Wang, *Dalton Trans.*, 2010, **39**, 6732; (*e*) W. J. Evans, J. R. Walensky and J. W. Ziller, *Organometallics*, 2010, **29**, 945; (*f*) W. J. Evans, J. R. Walensky, J. W. Ziller and A. L. Rheingold, *Organometallics*, 2009, **28**, 3350; (*g*) D. Baudry, A. Dormond and A. Hafid, *J. Organomet. Chem.*, 1995, **494**, C22.

3 (*a*) F. T. Edelmann, *Chem. Soc. Rev.*, 2012, **41**, 7657; (*b*) F. T. Edelmann, Homogeneous Catalysis Using Lanthanide Amidinates and Guanidinates, in *Structure and Bonding*, ed. P. W. Roesky, Springer, 2010, vol. 137, p. 109.

4 (*a*) W. Yi, J. Zhang, M. Li, Z. Chen and X. Zhou, *Inorg. Chem.*, 2011, **50**, 11813; (*b*) Y. Wu, S. Wang, L. Zhang, G. Yang, X. Zhu, Z. Zhou, H. Zhu and S. Wu, *Eur. J. Org. Chem.*, 2010, 326; (*c*) Z. Du, W. Li, X. Zhu, F. Xu and Q. Shen, *J. Org. Chem.*, 2008, **73**, 8966; (*d*) S. Zhou, S. Wang, G. Yang, Q. Li, L. Zhang, Z. Yao, Z. Zhou and H.-B. Song,

Organometallics, 2007, **26**, 3755; (*e*) W.-X. Zhang, M. Nishiura and Z. Hou, *J. Am. Chem. Soc.*, 2005, **127**, 16788.

5 (*a*) G. Himbert, W. Schwickerath and G. Maas, *Liebigs Ann. Chem.*, 1985, **7**, 1389; (*b*) G. Himbert and W. Schwickerath, *Liebigs Ann. Chem.*, 1984, **1**, 85; (*c*) H. Fujita, R. Endo, A. Aoyama and T. Ichii, *Bull. Chem. Soc. Jpn.*, 1972, **45**, 1846.

6 T.-G. Ong, J. S. O'Brien, I. Korobkov and D. S. Richeson, *Organometallics*, 2006, **25**, 4728.

7 (*a*) M. Arrowsmith and M. S. Hill, Alkaline Earth Chemistry: Applications in Catalysis, in *Comprehensive Inorganic Chemistry II*, ed. T. Chivers, Elsevier, 2013, vol. 1, p. 1189; (*b*) A. G. M. Barrett, M. R. Crimmin, M. S. Hill and P. A. Procopiou, *Proc. R. Soc. London, Ser. A*, 2010, **466**, 927; (*c*) M. R. Crimmin and M. S. Hill, Homogeneous Catalysis with Organometallic Complexes of Group 2, in *Topics in Organometallic Chemistry*, ed. S. Harder, 2013, vol. 45, p. 191; (*d*) S. Harder, *Chem. Rev.*, 2010, **110**, 3852.

8 A. G. M. Barrett, M. R. Crimmin, M. S. Hill, P. B. Hitchcock, S. L. Lomas, M. F. Mahon, P. A. Procopiou and K. Suntharalingam, *Organometallics*, 2008, **27**, 6300.

9 R. J. Schwamm and M. P. Coles, *Organometallics*, 2013, **32**, 5277.

10 T. M. Cameron, C.-Y. Xu, A. G. Dipasquale and A. L. Rheingold, *Organometallics*, 2008, **27**, 1596.

11 M. L. Cole and P. C. Junk, *New J. Chem.*, 2005, **29**, 135.

12 M. Arrowsmith, M. R. Crimmin, M. S. Hill, S. L. Lomas, D. J. MacDougall and M. F. Mahon, *Organometallics*, 2013, **32**, 4961.